Chemical Physics Letters 514 (2011) 251–256

Contents lists available at SciVerse ScienceDirect

Chemical Physics Letters

journal homepage: www.elsevier.com/locate/cplett

A sequential MC/TD-DFT study of the solvatochromic shift of the pyridinium-*N*-phenoxide betaine dye in water using standard and long-range corrected functionals

Leonardo B.A. Oliveira [a,1], Tertius L. Fonseca [a,*], Kaline Coutinho [b], Sylvio Canuto [b]

[a] Instituto de Física, Universidade Federal de Goiás, CP 131, 74001-970 Goiânia, GO, Brazil
[b] Instituto de Física, Universidade de São Paulo, CP 66318, 05314-970 São Paulo, SP, Brazil

ARTICLE INFO

Article history:
Received 19 July 2011
In final form 19 August 2011
Available online 24 August 2011

ABSTRACT

Solvatochromic shifts of the π–π^* and n–π^* transitions for the pyridinium-*N*-phenoxide [2-(pyridinium-1-yl)phenolate] betaine changing from vacuum to water, have been investigated using Monte Carlo simulations and time-dependent density functional theory schemes using standard and long-range corrected functionals. The classical Boltzmann distribution of the interring twist angle obtained from the calculated free energy agrees with a Car–Parrinello distribution. For the calculated spectral shifts BHandHLYP/6-311+G(2d,p) performs better than the CAM-B3LYP/6-311+G(2d,p) or LC-ωPBE/6-311+G(2d,p) model but the experimental shift is very well reproduced only after the inclusion of solute polarization and proper consideration of the twist geometry relaxation associated with the intramolecular charge transfer.

1. Introduction

The photophysics of the 2,6-diphenyl-4-(2,4,6-triphenylpyridinium-1-yl)phenolate [Reichardt dye or $E_T(30)$] has been a subject of great interest because of the exceptional large solvatochromism in the spectral region of the ultra-violet–visible (UV–Vis) in different solvents [1–6]. $E_T(30)$ is a sensitive solvatochromic molecule that can be used as a suitable spectroscopic probe to define a solvent polarity scale [1]. In this betaine dye a marked change in the dipole moment upon excitation makes the ground state more solvated than the excited state, resulting in a large blue shift that increases with increasing solvent polarity. Additionally, a great variety of pyridinium-*N*-phenolate betaine dyes with marked spectral properties have been synthesized by substitution of the peripheral phenyl groups of $E_T(30)$ [7]. In particular, interesting variants of $E_T(30)$ are the 2-(pyridinium-1-yl)phenolate (ortho-betaine, OB) and the 4-(pyridinium-1-yl)phenolate (para-betaine, PB) isomers. These betaine models possess a ground state characterized by a large value of the dipole moment due to a charge separation in the nitrogen (positive) and oxygen (negative) atoms. Experimental results of UV–Vis spectra of the OB and the PB in solutions reported by González et al. [8] have shown that it exhibits very prominent transition energy shifts in 12 solvents of different polarities, going from benzene (or toluene) to water. For OB, a large shift from benzene (λ_{max} = 528 nm = 18 940 cm^{-1} = 2.35 eV) to water (λ_{max} = 378 nm = 26 455 cm^{-1} = 3.28 eV), has been measured to be *ca.* 0.93 eV. And also, an estimation of 18 509 ± 1266 cm^{-1} = 2.29 ± 0.16 eV for the OB transition energy in vacuum was made by linear regression of McRae equation, giving a vacuum–water shift of 7946 ± 1266 cm^{-1} = 0.99 ± 0.16 eV. However, it was found that the isomer PB is sparingly soluble in solvent of low polarity [8]. For instance, it is not soluble in toluene, benzene, chloroform, dichloromethane and acetone. Although there are some theoretical results for PB in vacuum and in aqueous solution [9], there are no measurements or estimative of its electronic absorption transitions in low polarity solvents and in vacuum. Thus, the theoretical study of the solvatochromism of the isomer OB is more interesting due its interaction with a wide range of solvent in different polarity and a better understanding of the transition shift of this betaine model in aqueous solution is of essential importance to understand more complexes dyes.

In recent years there are some theoretical investigations on electronic transitions and structural changes of OB in water [10–13]. In the first theoretical work of OB [10], it was shown that in vacuum this dye possesses a twisted ground-state geometry with a torsion angle, φ, between the phenoxide and the pyridinium rings around 30°, but in aqueous solution this torsion angle increases to around 60°. This conclusion was based on the free energy profile for φ varying from 0° to 90° with interval of 7.5° in classical Monte Carlo (MC) simulations. This relaxation effect in geometry was associated with an intramolecular charge redistribution that changes the dipole moment, μ, from *ca.* 7.1 D (in vacuum with φ = 30°) to *ca.* 8.2 D

* Corresponding author. Fax: +55 62 3512 1014.
E-mail address: tertius@if.ufg.br (T.L. Fonseca).
[1] Permanent address: CEPAE, Universidade Federal de Goiás, CP 131, 74001-970 Goiânia, GO, Brazil.

0009-2614 © 2011 Elsevier B.V. Open access under the Elsevier OA license.
doi:10.1016/j.cplett.2011.08.056

(in vacuum with $\varphi = 60°$) calculated with MP2/6-31G level. Considering the explicit hydration effect and the unpolarized charge redistribution of the most probable geometry of OB in water ($\varphi = 60°$ and $\mu = 10.8$ D), it was obtained a vacuum–water shift of 1026 ± 69 cm^{-1} = 0.13 ± 0.01 eV for the π–π^* transition and 6060 ± 89 cm^{-1} = 0.75 ± 0.01 eV for the n–π^* transition using the semiempirical method ZINDO/CIS [10]. Later on, it was shown that another important aspect for a better description of the solvatochromism of the OB dye in water is the solute polarization due to the presence of the solvent [12], which can be included in a precise way using an iterative and sequential quantum mechanics/classical mechanics (S-QM/MM) procedure [14]. This solute polarization in aqueous solution increases the dipole moment of *ca.* 50% (from 8.2 to 12.3 D both values in geometry of OB with $\varphi = 60°$) and *ca.* 75% compared with the vacuum situation (7.1 D in geometry of OB with $\varphi = 30°$) obtained with MP2/cc-pVDZ [12]. Then using this classical polarized model of OB in water ($\varphi = 60°$ and $\mu = 12.3$ D), it was obtained a shift of 6360 ± 100 cm^{-1} = 0.79 ± 0.01 eV for the n–π^* using ZINDO/CIS [12]. In a subsequent work, Murugan and Ågren [13] analyzed the flexibility, the charge redistribution and the shift of the n–π^* and π–π^* transitions of OB in vacuum and in aqueous solution using a Car–Parrinello mixed molecular mechanics (CP-QM/MM) procedure combined with the semiempirical INDO/CIS method to calculate the transition energies. They found that the OB dye is very flexible with respect to the torsion angle between the phenoxide and the pyridinium rings presenting a twist amplitude of ±30° around 30° in vacuum and 55.6° in aqueous solution. These CP-QM/MM calculations corroborate our previous result that the most probable geometry of OB in vacuum is with the torsion angle in 30° and around 60° in water [10]. However, they stressed that the twist amplitude is large and it can not be neglected. They estimated the dipole moment of 6.2 D in vacuum and 13.3 D in water, compatible with our previous values of 7.1 and 12.3 D, respectively with MP2/ccp-VDZ [12]. They calculated the total charge on the rings and obtained −0.53 and −0.73 *e* for the phenoxide ring in vacuum and in water, respectively, in good concordance with our corresponding values of −0.535 and −0.738 *e*. In addition, they obtained a shift of 7448 cm^{-1} = 0.92 eV for the π–π^* transition and 10 346 cm^{-1} = 1.28 eV for the n–π^* transition that are in very good agreement with the experimental results of benzene–water shift as 0.93 eV for the π–π^* transition or the estimated vacuum–water shift of 0.99 ± 0.16 eV [8]. Within this hybrid QM/MM framework, the time-dependent density functional theory (TD-DFT) approach [15] using long-range corrected (LR) functionals have been used in the calculations of excitation energies, polarizabilities, and other properties [16–18].

To the best of our knowledge, there is one theoretical investigation [11] on the excitation energies of OB using the TD-DFT approach in conjunction with the standard B3LYP functional [19,20] and the 6-311G(d) basis set that presents a calculated value of 0.17 eV for vacuum–water shift of the transitions energy and it is in discrepancy with the experimental result [8].

In this Letter, we extend our previous calculations [10,12] of the absorption spectra of OB in water and its solvatochromic shift of the π–π^* and n–π^* transitions compared to the vacuum situation using TD-DFT schemes considering a classical model of the OB that includes the geometry relaxation, intramolecular charge transfer and polarization due to the presence of the solvent. We also show that the classical Boltzmann distribution for the torsion angle φ obtained from the calculated Helmholtz free energy is in agreement with the previously obtained Car–Parrinello distribution [13]. We investigate the performance of standard and LR functionals in predicting the charge-transfer excited states of OB in presence of water molecules treated as point charges using sequentially MC simulations and TD-DFT (S-MC/TD-DFT) calculations [21–23]. TD-DFT schemes have been widely used for evaluating excited state energies but the selection of exchange–correlation functional is a prerequisite to obtain reliable predictions of these electronic properties. It is well known that standard functionals fail to describe charge-transfer states because of the incorrect asymptotic behavior of the exchange interaction [24,25]. Long-range corrected functionals, such as CAM-B3LYP (CAM-B3LYP: Coulomb-attenuating method applied to B3LYP) of Yanai et al. [26] and LC-ωPBE (LC: long-range correction) of Vydrov et al. [27], improve this asymptotic behavior and thus they may provide a reliable description of these electronic states. Here, the average solvent electrostatic configuration (ASEC) procedure [28] has been used to obtain statistically converged results for the absorption spectra of the OB embedded in electrostatic polarization field of water molecules treated as point charges.

2. Calculation details

A sequential S-MC/TD-DFT methodology [21–23] has been applied to study the absorption spectra of hydrated OB. The MC simulations were carried out with the DICE program [29] using the Metropolis sampling, for 1 OB and 900 water molecules, in the canonical NVT ensemble in a cubic box with periodic boundary conditions [30]. The intermolecular interaction is described by the Lennard–Jones (LJ) plus Coulomb potential with 3 parameters for each interacting site. For the water molecules, we have used the simple point charges (SPC) model proposed by Berendsen et al. [31]. For the solute, the LJ parameters were obtained combining the OPLS parameters of the phenol [32] and the pyridine [33] as before [10,12]. The atomic charges used in the Coulomb potential were obtained using the CHELPG electrostatic mapping [34] at the second-order Møller–Plesset perturbation theory (MP2) level with the cc-pVDZ basis set, as implemented in GAUSSIAN 03 program [35]. In all simulations the thermalization stage comprises 2.7×10^7 MC steps and is followed by the average stage of 1.8×10^8 MC steps. A more detailed description of the simulation procedure used here is given elsewhere [10,12].

The inclusion of polarization effects plays a central role in theoretical studies of solvent effects [36–38]. In a previous work [12], we have iteratively applied the S-MC/MP2 methodology and used the ASEC to calculate the dipole moment of the conformer (with torsion angle of $\varphi = 60°$, see Table 1 of Ref. [12]) in the presence of the water molecules. It is found, for this polarized conformer in-solution, a dipole moment value of 12.3 D (obtained at the MP2/cc-pVDZ level of theory) that is *ca.* 75% larger than the vacuum result [12]. Here, in order to analyze the influence of the torsion angle on the in-solution dipole moment, we have performed a series of MC simulation with the conformers of OB in the rigid geometry but varying the torsion angle from 0° to 90° with interval of 7.5°. The conformer geometries used in MC simulations were obtained by previous optimization in vacuum at the MP2/6-31G level of calculation [10]. The dipole moment of each conformation were obtained with MP2/cc-pVDZ calculations on the ASEC bearing conformers of OB electrostatically embedded in 320 water molecules of 100 uncorrelated configurations (having less than 10% of statistical correlation), giving a total of 96 000 point charges (= 3 atoms × 320 molecules × 100 configurations). The statistically converged dipole moment values for the OB conformers are reached in five iterations, similar to the iterative process reported in Ref. [12].

The most important geometry relaxation of OB in water is the torsion angle. The Helmholtz free energy (ΔG) calculations reported in a previous work [10] have shown that the most stable angle φ for the unpolarized model of the OB in water is 60°. An important point is whether the solute polarization effect will change the result for the stability of the torsion angle. Following a previous work, we have applied the free energy perturbation (FEP) [39–41] as implemented in the DICE program [29] to calculate the ΔG for the polarized model of OB in aqueous solution as

function of the angle φ. All the simulation protocol and parameters, except the solute atomic charges, used for ΔG calculations were those already reported in a previous work [10].

The excitation energies were obtained using the TD-DFT [15] with several different exchange–correlation functionals. We have used three standard functionals: B3LYP [19,20], PBE1PBE [42] and BHandHLYP [43]. These standard functionals have percentages of Hartree–Fock exchange that amounts to 20%, 25%, and 50%, respectively. Additionally, we used two LR functionals: the CAM-B3LYP [26], and the LC-ωPBE [27]. In these two latter functionals the asymptotic behavior of the exchange interaction is improved partitioning it into short- and long-range components. We have used in all TD-DFT calculations the 6-311+G(2d,p) basis set that provides converged electronic transition results for a number of solvated organic molecules [44,45]. Also, the OB was embedded in the electrostatic field of the aqueous environment through the ASEC with 96 000 point charges. All TD-DFT calculations were made using the Gaussian 03 program [35], except for the LR–TD-DFT calculations that were carried out with the Gaussian 09 [46].

3. Results and discussion

The dipole moments of the OB in vacuum and in aqueous solution are obtained with MP2/cc-pVDZ calculations. The calculated values are shown in Figure 1. As it can be seen, in vacuum the intramolecular charge transfer between the phenoxide and pyridinium rings is very sensitive to the twist motion between them and the dipole moment can increase up to *ca.* 40% (from 6.6 D in $\varphi = 0°$ to 9.2 D in $\varphi = 82.5°$). The dipole moment of OB in vacuum for the conformers with $\varphi = 30°$ and 60° are 7.1 and 8.2 D, respectively. However, in aqueous solution, the dipole moment is much large ($\approx$12 D) but less sensitive to the twist motion between the rings. It increases only *ca.* 7% (from 11.6 D $\varphi = 0°$ to 12.4 D $\varphi = 67.5°$). The dipole moment of polarized OB in water for the conformers with $\varphi = 30°$ and 60° are 11.7 and 12.2 D, respectively. For comparison, the polarized dipole moment values calculated with the polarized continuum model (PCM) [47], as implemented in Gaussian 03 program, are 11.0 and 11.6 D for $\varphi = 30°$ and 60°, respectively, using the same level of theory. These values also present a small increase of *ca.* 5%.

Using the atomic charges set for each torsion angle φ that represents the polarized OB in water, the $\Delta G(\varphi)$ profile was obtained. The calculated values are shown in Figure 2. For comparison we also present the vacuum profile obtained with MP2/cc-pVDZ model and the aqueous solution profile obtained with the unpolarized model of OB previously calculated in Ref. [10]. As it can be seen, the ΔG profiles for the angle φ of OB in water are similar considering the classical unpolarized and polarized models of OB. Probably the gain of energy in the dipole–dipole solute–solvent (OB–water) interaction is lost in the solvent–solvent (water–water) reorganization around the solute (OB). The most important difference appears for torsion angles larger than 60°. While the unpolarized OB presents a flat ΔG profile between 60° and 90° (with a difference smaller than 0.5 kcal/mol), the polarized OB presents a most stable conformer in 60° and an increasing barrier with a maximum at 90° (now the ΔG barrier between 60° and 90° is *ca.* 2.7 kcal/mol). These results are in very good agreement with CP-QM/MM calculations (see Fig. 3 of Ref. [13]), where the probability distribution of the torsion angle of OB in water presents two maxima, around 60° and 120°, and a minimum in 90°. Thus, the Car–Parrinello distribution confirms the existence of a free energy barrier in 90°. Note that, the inclusion of the polarization effect of OB in water does not change the previous conclusion that the most stable conformation of OB in water is with $\varphi = 60°$. The question of the amplitude of values obtained for the angle φ can also be addressed from the classical simulation. The probability of the conformation for a specific torsion angle φ_i, can be obtained from the normalized Boltzmann distribution:

$$P(\varphi_i) = \frac{\exp(-G(\varphi_i)/kT)}{\sum_i \exp(-G(\varphi_i)/kT)} = \frac{\exp(-G(\varphi_i)/kT)}{Z},$$

where $G(\varphi_i)$ is the relative free energy for the angle φ_i, with $G(0) = 0$, kT is the thermal energy and Z is the normalization constant obtained by the sum over all used φ_i. These two normalized distributions for torsion angle of OB in vacuum and in water are shown in the insert of Figure 2. Comparing these distributions with the obtained with CP-QM/MM simulations [13], it is noted an excellent agreement. The amplitude is around ±30° with a maximum in 30° for OB in vacuum and in 55° for the OB in water.

All TD-DFT calculations performed here predict the first excited state as an intense π–π^* transition, responsible by the optical properties of this compound, and the second excited state as a weak n–π^*

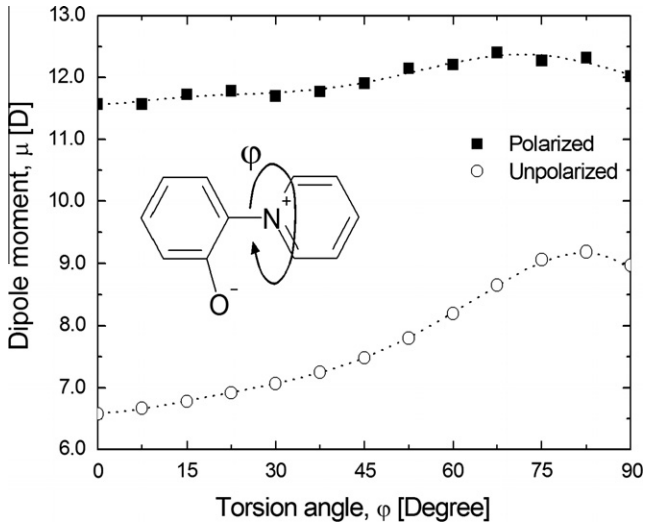

Figure 1. Dipole moment (in D) of OB in vacuum (open circle) and in aqueous solution (filled square) as a function of the torsion angle φ between the phenoxide and pyridinium rings using MP2/cc-pVDZ level of calculation.

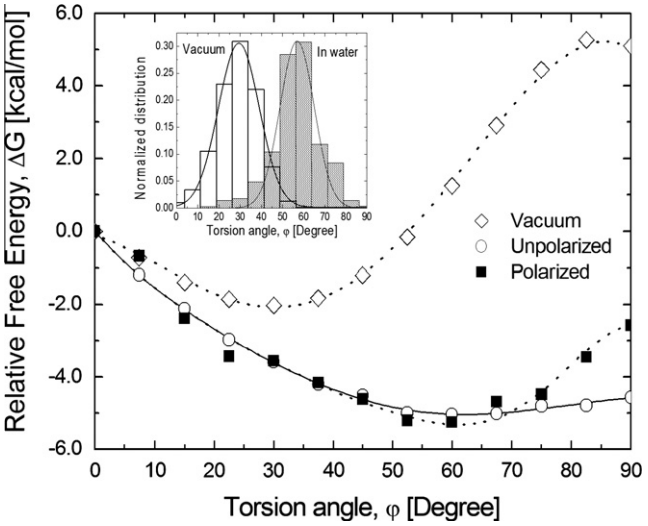

Figure 2. Relative Helmholtz free energy ΔG as a function of the torsion angle φ between the phenoxide and pyridinium rings using MP2/cc-pVDZ level of calculation for the vacuum situation and free energy perturbation for the classical unpolarized and polarized models of OB in water. It is shown in the insert the normalized Boltzmann distribution of the torsion angle of OB in vacuum and in polarized OB in water.

transition in vacuum ($\varphi = 30°$) and in water ($\varphi = 60°$). The exception is the TD-BHandHLYP results that predict the n–π^* transition as third and fifth transitions in vacuum and in water, respectively. Also, all TD-DFT calculations indicate that the π–π^* state originates mainly from a HOMO → LUMO excitation whereas the n-π^* state corresponds to HOMO-1 → LUMO excitation, except for the TD-BHandHLYP calculations that give the n–π^* state consisting of about equal contributions of HOMO-1 → LUMO and HOMO-2 → LUMO excitations. The shapes of the frontier orbitals involved in the lowest-lying π–π^* transition are illustrated in Figure 3. One can see that the HOMO orbital is delocalized over the phenoxide ring and that upon excitation, the shape of the LUMO orbital corresponds to an intramolecular charge transfer from phenoxide donor ring to the pyridinium acceptor ring. This description of the frontier HOMO and LUMO molecular orbitals is in agreement with the results obtained with CASSCF level for the PB isomer in water [9].

TD-DFT absorption energy results for the π–π^* and n–π^* transitions obtained with the standard and LR functionals using the 6-311+G(2d,p) basis set in vacuum and in water solution are presented in Table 1. In vacuum ($\varphi = 30°$), the B3LYP and (PBE1PBE) results give the first transition with energies of 2.02 and (2.11 eV). Thus, both the TD-DFT models predict for the π–π^* transition underestimated energy values compared with the experimental result of 2.35 eV in benzene and 2.29 ± 0.16 eV in vacuum [8]. The CAM-B3LYP gives an absorption energy of 2.38 eV for the intense π–π^* transition in very good agreement with the experiment, in analogy with other studies [17,48]. The LC-ωPBE gives an overestimated result of 2.69 eV. It should be stressed that the BHandHLYP result obtained for the π–π^* transition is 2.46 eV slightly larger than the corresponding experimental one. All TD-DFT calculations show that the n–π^* transition takes place at higher energy region of 2.58–3.66 eV, in comparison with the experimental result [8]. In vacuum, the largest energy value predicted by the BHandHLYP functional for the n–π^* transition is related to a reversal of the relative location of the lowest-lying excited states and the n–π^* transition is predicted to be the third transition.

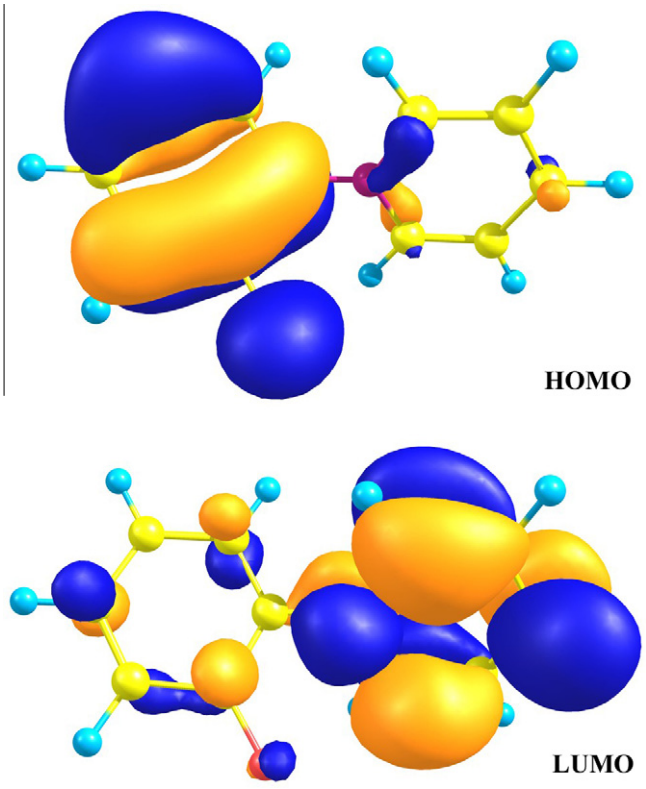

Figure 3. The frontier molecular orbitals of OB in water indicating the charge transfer excitation of the π–π^* transition from the phenoxide ring to pyridinium ring.

Now, we compare our TD-DFT results for the π–π^* and n–π^* transitions in liquid phase with the available experimental data (see Table 1). We have considered both the unpolarized and polarized situations in order to estimate the influence of polarization effects on the absorption spectra of OB in aqueous solution. Each result obtained in solution represents a statically converged result obtained with the ASEC procedure. In aqueous solution ($\varphi = 60°$), the B3LYP value of the π–π^* transition energy for the polarized (unpolarized) OB is of 2.55 eV (2.13 eV). The corresponding energy result obtained using PBE1PBE is of 2.46 eV (2.10 eV). In comparison with the experimental result of 3.28 eV in water [8], these standard functionals predict for π–π^* transition underestimated energy values. Thus these standard functionals provide for the polarized OB excitation energies only qualitative accord with the experiment. These findings are in line with a previous study of Caricato et al. [11] for the π–π^* excited state of OB in water using a TD-DFT method in combination with the PCM. For comparison the PCM-TD-B3LYP/6-311+G(d) model gives for the most stable conformer an energy value of 2.25 eV. As expected, the CAM-B3LYP functional performs better than B3LYP giving an absorption energy of 2.96 eV for the intense π–π^* transition but that is still smaller than the corresponding experimental 3.28 eV. In contrast, the LC-ωPBE functional gives an overestimated value of 3.45 eV. This later result is in better agreement with the experiment. But differently of their standard congeners, the experimental value of the excitation energy is well reproduced by the BHandHLYP model after the inclusion of the polarization effect. For the polarized OB, the BHandHLYP result obtained for the π–π^* transition is of 3.36 eV, being only 0.08 eV larger than the corresponding experimental one. Note that the unpolarized results predicted for the π–π^* transition is somewhat too small (see Table 1), indicating that the solute polarization effects are thus very important for the reliable description of this excitation energy as already shown by other molecular systems [49,50]. With the exception of the PBE1PBE functional, all TD-DFT calculations show that the energies of the n–π^* transition of polarized OB takes place in the higher energy region of 3.72–5.07 eV, beyond the experimental report [8]. This indicates that the n–π^* transition is also subjected to a large spectral shift but was undetected experimentally, where the large reported shift is due to the π–π^* transition.

We discuss the TD-DFT solvatochromic shift of the π–π^* and n–π^* transitions in changing from vacuum to water. The solvation shift includes both the geometry relaxation and polarization of the solute due to the solvent. Experimentally, the vacuum UV/Vis absorption spectrum of OB has an estimated value at 2.29 ± 0.16 eV, which is blue-shifted in aqueous solution to 3.28 eV [8]. Hence a very large experimental solvatochromic shift of 0.99 ± 0.16 eV is observed. In Table 1, the B3LYP (PBE1PBE) functional predicts for the π–π^* transition energy an expected substantial blue shift estimated in 0.53 (0.35 eV) but it is very small when compared with the experimental shift. The CAM-B3LYP functional gives a blue shift of 0.58 eV, that is slightly larger than that obtained with the B3LYP. The LC-ωPBE functional predicts a better solvation shift of 0.75 eV for the π–π^* transition. It is interesting to note that the agreement with experiment is further improved with the BHandHLYP functional. This latter functional performs better than CAM-B3LYP and LC-ωPBE, and provides a solvatochromic shift of 0.90 eV for the π–π^* transition of polarized OB. For comparison the polarization effects provide a significant increase in the solvation shift of 0.42, 0.36, 0.48, 0.40 and 0.38 eV for B3LYP, PBE1PBE, BHandHLYP, CAM-B3LYP and LC-ωPBE, respectively. It is noted that the calculations also indicate a large solvation blue shift for the n–π^* transition, with similar charge

Table 1
Excitation energies (in eV) for the π–π^* and n–π^* of the OB in vacuum and in aqueous solution. The vacuum–water shifts are also shown in parenthesis. All results were obtained using the 6-311+G(2d,p) basis set.

	Vacuum (φ = 30°)		In water (φ = 60°)			
			Unpolarized		Polarized	
	π–π^*	n–π^*	π–π^*	n–π^*	π–π^*	n–π^*
B3LYP	2.02	2.58	2.13 (0.11)	3.10 (0.52)	2.55 (0.53)	3.72 (1.14)
PBE1PBE	2.11	2.71	2.10 (−0.01)	2.78 (0.07)	2.46 (0.35)	3.13 (0.42)
BHandHLYP	2.46	3.62	2.88 (0.42)	4.50 (0.88)	3.36 (0.90)	5.07 (1.45)
CAM-B3LYP	2.38	3.21	2.56 (0.18)	3.46 (0.25)	2.96 (0.58)	3.84 (0.63)
LC-ωPBE	2.69	3.66	3.07 (0.38)	4.07 (0.41)	3.45 (0.76)	4.41 (0.75)
Exp.[a]	2.35 in benzene				3.28 (0.93)	
	2.29 ± 0.16 in vacuum				3.28 (0.99 ± 0.16)	

[a] Experimental absorptions (in eV) from Ref. [8].

Table 2
Excitation energies and the vacuum–water shifts (in eV) for the π–π^* transition of the OB as function of the torsion angle φ most probable. All results were obtained using the 6-311+G(2d,p) basis set. The vacuum–water shifts were calculated in relation to the most probable vacuum transition energies of 2.02 ± 0.17 eV and 2.46 ± 0.14 eV obtained with B3LYP and BHandHLYP, respectively. Here, the deviations represent the changes in the transition energy due to the twist motion between the rings in vacuum.

φ (°)	Vacuum		In water		Vacuum–water shift	
	B3LYP	BHandHLYP	B3LYP	BHandHLYP	B3LYP	BHandHLYP
15.0	2.17	2.56				
22.5	2.09	2.51				
30.0	2.02	2.46				
37.5	1.94	2.39				
45.0	1.84	2.31	2.59	3.28	0.57 ± 0.17	0.82 ± 0.14
52.5			2.57	3.33	0.55 ± 0.17	0.87 ± 0.14
60.0			2.54	3.36	0.52 ± 0.17	0.90 ± 0.14
67.5			2.48	3.37	0.46 ± 0.17	0.91 ± 0.14
75.0			2.43	3.36	0.41 ± 0.17	0.91 ± 0.14
82.5			2.45	3.44	0.43 ± 0.17	0.98 ± 0.14
Exp.[a]	2.35 in benzene		3.28		0.93	
	2.29 ± 0.16 in vacuum				0.99 ± 0.16	

[a] Experimental absorptions (in eV) from Ref. [8].

transfer. For instance, BHandHLYP gives a larger blue shift of 1.45 eV. But because of its low intensity this n–π^* transition is more difficult to be seen in the experiments.

We have also analyzed the influence of the water-induced geometrical changes on the solvatochromic shift of the π–π^* transition in water. Table 2 presents BHandHLYP and B3LYP results for the solvation shifts obtained for OB conformations varying the torsion angle within the most probable region of the twist motion between the rings presented in the insert of Figure 2, i.e. in-vacuum from 15° to 45° and in-water from 45° to 82.5°. It found that the impact of the increase of the torsion angle is more relevant on the transition energies obtained in vacuum than in water. For torsion angles with values between 15° and 45°, the vacuum BHandHLYP (B3LYP) results give the π–π^* transition in the energy region of 2.56–2.31 eV (2.17–1.84 eV). This leads to the most probable transition of 2.46 eV (2.02 eV) with variation of ±0.14 eV (±0.17 eV). In water for the torsion angle with values between 45° and 82.5° the corresponding energy region is of 3.28–3.44 eV (2.59–2.45 eV). This leads to the most probable transition of 3.36 eV (2.55 eV) with variation of ±0.06 eV (±0.07 eV). Thus, an interesting aspect of the BHandHLYP results shown in Table 2 is that the large solvation shifts of OB in water show a relatively small dependence with the torsion angle suggesting that the rigid-body approximation for the OB molecules, as used in Ref. [12], is appropriate to describe the most probable shift of 0.90 eV with TD-BHandHLYP/6-311+G(2d,p) in comparison with the maximum energy transition shift measured as 0.93 eV for benzene–water and estimated as 0.99 ± 0.16 eV for vacuum–water [8]. But of course, it is not suitable to describe the spectral broadening associated to the fluctuations around the most probable value of the twist angle and some other possible contributions related to the internal relaxation that we are not considering.

4. Conclusion

Using MC simulations and TD-DFT calculations we have presented a study of the excitation energies of the ortho-betaine in vacuum and water. We address the distribution of the interring twist angle in water and we reproduce a Car–Parrinello distribution using a classical Boltzmann approach from the Helmholtz free energy calculations. We compared results for the spectral shift obtained on statistically uncorrelated configurations with classical unpolarized and polarized models of OB using long-range corrected functionals (CAM-B3LYP and LC-ωPBE) and with standard ones (B3LYP, PBE1PBE, and BHandHLYP). All TD-DFT calculations give the π–π^* transition as the responsible by the optical properties of OB, but a large solvatochromic shift is also calculated for the n–π^* transition. It is found that the overall performance of the BHandHLYP is better than the CAM-B3LYP or LC-ωPBE in predicting the experimental solvation shift of the ortho-betaine in water. For the classical polarized model of the OB, the BHandHLYP/6-311+G(2d,p) model gives a solvatochromic shift of 0.90 eV, in good agreement with the experimental results of 0.93 eV for benzene–water and 0.99 ± 0.16 eV for vacuum–water, whereas the CAM-B3LYP and LC-ωPBE models with 6-311+G(2d,p) basis set provide underestimated solvation shifts of 0.58 and 0.76 eV, respectively.

Acknowledgments

This work has been partially supported by CNPq, CAPES, FAPESP, NBioNet and INCT-FCx (Brazil).

References

[1] C. Reichardt, Solvent Effects in Organic Chemistry, Verlag Chemie, Weinheim, New York, 1979.
[2] M.S. Paley, E.J. Meehan, C.D. Smith, F.E. Rosenberger, S.C. Howard, J.M. Harris, J. Org. Chem. 54 (1989) 3432.
[3] J.G. Dawber, S. Etemad, M.A. Beckett, J. Chem. Soc. Faraday Trans. 86 (1990) 3725.
[4] D.V. Matyushov, R. Schmid, B.M. Ladanyi, J. Phys. Chem. B 101 (1997) 1035.
[5] S.R. Mente, M. Maroncelli, J. Phys. Chem. B 103 (1999) 7704.
[6] M. Caricato, B. Mennucci, J. Tomasi, Mol. Phys. 104 (2006) 875.
[7] V. Kharlanov, W. Rettig, J. Phys. Chem. A 113 (2009) 10693.
[8] D. González, O. Neilands, M.C. Rezende, J. Chem. Soc. Perkin Trans. 2 (1999) 713.
[9] T. Ishida, P. Rossky, J. Phys. Chem. B 112 (2008) 11353.
[10] M.Z. Hernandes, R. Longo, K. Coutinho, S. Canuto, Phys. Chem. Chem. Phys. 6 (2004) 2088.
[11] M. Caricato, B. Mennucci, J. Tomasi, J. Phys. Chem. A 108 (2004) 6248.
[12] T.L. Fonseca, K. Coutinho, S. Canuto, Chem. Phys. 349 (2008) 109.
[13] N.A. Murugan, H. Ågren, J. Phys. Chem. A 113 (2009) 2572.
[14] H.C. Georg, K. Coutinho, S. Canuto, Chem. Phys. Lett. 429 (2006) 119.
[15] E. Runge, E.K.U. Gross, Phys. Rev. Lett. 52 (1984) 997.
[16] N.A. Murugan, J. Kongsted, Z. Rinkevicius, H. Ågren, Proc. Natl. Acad. Sci. U. S. A. 107 (2010) 16453.
[17] N.A. Murugan, J. Kongsted, Z. Rinkevicius, K. Aidas, H. Ågren, J. Phys. Chem. B 114 (2010) 13349.
[18] N.A. Murugan, J. Kongsted, Z. Rinkevicius, K. Aidas, K.V. Mikkelsenc, H. Ågren, Phys. Chem. Chem. Phys. 13 (2011) 12506.
[19] C. Lee, W. Yang, R.G. Parr, Phys. Rev. B 37 (1988) 785.
[20] A.D. Becke, J. Chem. Phys. 98 (1993) 5648.
[21] K. Coutinho, S. Canuto, J. Chem. Phys. 113 (2000) 9132.
[22] S. Canuto, K. Coutinho, M.C. Zerner, J. Chem. Phys. 112 (2000) 7293.
[23] R. Rivelino, K. Coutinho, S. Canuto, J. Phys. Chem. B 106 (2002) 12317.
[24] A. Dreuw, M. Head-Gordon, J. Am. Chem. Soc. 126 (2004) 4007.
[25] D.J. Tozer, R.D. Amos, N.C. Handy, B.O. Roos, L. Serrano-Andres, Mol. Phys. 97 (1999) 859.
[26] T. Yanai, D.P. Tew, N.C. Handy, Chem. Phys. Lett. 393 (2004) 56.
[27] O.A. Vydrov, J. Heyd, V. Krukau, G.E. Scuseria, J. Chem. Phys. 125 (2006) 074106.
[28] K. Coutinho, H.C. Georg, T.L. Fonseca, V. Ludwig, S. Canuto, Chem. Phys. Lett. 437 (2007) 148.
[29] K. Coutinho, S. Canuto, DICE: A Monte Carlo Program for Molecular Liquid Simulation, University of São Paulo, version 2.9, São Paulo, 2009.
[30] M.P. Allen, D.J. Tildesley, Computer Simulation of Liquids, Clarendon Press, Oxford, 1987.
[31] H.J.C. Berendsen, J.P.M. Postma, W.F. van Gunsteren, J. Hermans, in: B. Pullman (Ed.), Intermolecular Forces, Reidel, Dordrecht, 1981, p. 331.
[32] W.L. Jorgensen, T.B. Nguyen, J. Comput. Chem. 14 (1993) 195.
[33] W.L. Jorgensen, J.M. Briggs, M.L. Contreras, J. Phys. Chem. 94 (1990) 1683.
[34] C.M. Breneman, K.B. Wiberg, J. Comput. Chem. 11 (1990) 361.
[35] M.J. Frisch et al., Gaussian 03, Revision D.01, Gaussian, Inc., Wallingford CT, 2004.
[36] A. Wallqvist, P. Ahlström, G. Karlstrom, J. Phys. Chem. 94 (1990) 1649.
[37] C.J. Cramer, D.G. Truhlar, Science 256 (1992) 213.
[38] W.L. Jorgensen (Ed.), J. Chem. Theor. Comput. 3(6) (2007) 1877–2145.
[39] R.W. Zwanzig, J. Chem. Phys. 22 (1954) 1420.
[40] W.L. Jorgensen, C. Ravimohan, J. Chem. Phys. 83 (1985) 3050.
[41] W.L. Jorgensen, L.L. Thomas, J. Chem. Theor. Comput. 4 (2008) 869.
[42] J.P. Perdew, K. Burke, M. Ernzerhof, Phys. Rev. Lett. 77 (1996) 3865.
[43] A.D. Becke, Phys. Rev. A 38 (1988) 3098.
[44] J. Preat, P.-F. Loos, X. Assfeld, D. Jacquemin, E.A. Perpète, Int. J. Quantum Chem. 107 (2007) 574.
[45] T.L. Fonseca, H.C.B. de Oliveira, M.A. Castro, Chem. Phys. Lett. 457 (2008) 119.
[46] M. J. Frisch et al., Gaussian 09, Revision A.02, Gaussian, Inc., Wallingford CT, 2009.
[47] J. Tomasi, B. Mennucci, R. Cammi, Chem. Rev. 105 (2005) 2999.
[48] D. Jacquemin, E.A. Perpète, G.E. Scuseria, I. Ciofini, C. Adamo, J. Chem. Theor. Comput. 4 (2008) 123.
[49] H.C. Georg, K. Coutinho, S. Canuto, J. Chem. Phys. 126 (2007) 034507.
[50] T.L. Fonseca, H.C. Georg, K. Coutinho, S. Canuto, J. Phys. Chem. A 113 (2009) 5112.